An *in situ* Transmission Electron Microscopy Study of the Ion Irradiation Induced Amorphisation of Silicon by He and Xe

PD Edmondson[1,*], KJ Abrams[2], JA Hinks[3], G Greaves[3], CJ Pawley[3], I Hanif[3] and SE Donnelly[3]

[1]*Materials Science & Technology Division, Oak Ridge National Laboratory, Oak Ridge, TN 37831. USA*

[2]*Schools of Materials Science and Engineering, University of Sheffield, Sheffield, S13JD UK*

[3]*School of Computing and Engineering, University of Huddersfield, Huddersfield, HD1 3DH. UK*

Transmission electron microscopy with *in situ* ion irradiation has been used to examine the ion-beam-induced amorphisation of crystalline silicon under irradiation with light (He) and heavy (Xe) ions at room temperature. Analysis of the electron diffraction data reveal the heterogeneous amorphisation mechanism to be dominant in both cases. The differences in the amorphisation curves are discussed in terms of intra-cascade dynamic recovery, and the role of electronic and nuclear loss mechanisms.

Keywords: ion irradiation, silicon, amorphisation, in situ TEM

Corresponding author: Philip Edmondson (edmondsonpd@ornl.gov)

The fabrication of modern semiconductor devices involves upwards of 100 processing steps including ion implantation which is commonly used to introduce dopants to the material. However, an unwanted side effect of implantation is the introduction of lattice damage which must be removed through annealing. To date, the response of crystalline silicon to ion irradiation (i.e. ion mass, energy, temperature, fluence effects) has been well researched and is, as such, considered well understood. However, the fundamental mechanisms by which the material is rendered amorphous are less understood.

Many models for the amorphisation of materials under ion irradiation exist (see, for example, references [1-3]) and it is assumed that there are two basic mechanisms: *heterogeneous* and *homogeneous*. Generally, the homogeneous mechanism is assumed to be dominant during light ion irradiation and the heterogeneous mechanism during heavy ion irradiation [1-3]. Homogeneous nucleation assumes that there is an accumulation of defects within the lattice that at some point becomes unstable (i.e. a high energy state) and the lattice collapses to a more stable (i.e. a lower energy state) amorphous phase [4-6]. Conversely, heterogeneous nucleation – first proposed by Morehead and Crowder [7] – assumes that small pockets of amorphous material are formed by the incoming ions and that the overlapping of these damage zones lead to the formation of an amorphous layer as described by Equation 1:

$$f_a = 1 - e^{-V.D} \tag{1}$$

Where f_a is the amorphous fraction, V is the average damage volume per ion and D is the dose (ions per unit volume). This model for heterogeneous amorphisation was extended further by Gibbons to allow for the possible requirement for overlapping of collision cascades to amorphise the substrate as described by Equation 2 [8]:

$$f_a = 1 - \sum_{k=0}^{m-1} \frac{(V.D)^k}{k!} e^{-V.D} \quad (2)$$

where m is the number of overlapping cascades required to render a volume amorphous. It should be noted that in the case of direct-hit amorphisation, that is, amorphisation which occurs within a single collision cascade (i.e. no cascade overlaps are required) equation 2 reduces to equation 1.

A kinetic theory of amorphisation based on the Avrami-Johnson-Mehl (AJM) model has also been successfully applied to describe ion-beam-induced amorphisation of Si and is described through equation 3:

$$f_a = 1 - e^{(-K.D^n)} \quad (3)$$

where K is a temperature dependent parameter and n is an exponent describing three-dimensional growth. It had previously been assumed that within the confines of a collision cascade the material is always rendered amorphous thus producing spatially isolated amorphous zones [9-11]. Recent work on the annealing of damage created by individual collision cascades [9, 12], cascade overlaps [2] and cluster/molecular ion irradiation [13, 14] has indicated that this may not necessarily be true with the cascade volumes consisting of variable levels of damage ranging from dilute up to completely amorphous.

Understanding the formation, recovery and stability of damage produced within the confines of individual collision cascades is of significant importance in the elucidation of operative amorphisation mechanisms – particularly when trying to determine the role of ion mass and the contribution of nuclear/electronic energy loss processes.

Transmission electron microscopy (TEM) samples were prepared from {001} Czochralski-grown silicon wafers, mechanically thinned and then ion polished to electron transparency. Specimens were then ion irradiated to amorphisation at room temperature *in situ* within a JEOL

JEM-2000FX TEM at the Microscope and Ion Accelerator for Materials Investigation (MIAMI) facility at the University of Huddersfield [15] using 30 keV He^+ or 80 keV Xe^+ ions. The He ion energy was chosen such that the damage profile throughout the thickness of the TEM specimen was approximately uniform whilst minimising implantation of He (<0.05% of the fluence). The Xe ion energy was chosen to produce a damage profile approximately 50 nm in thickness. Damage injection rates, damage profiles and ion ranges were calculated using the Stopping and Ranges of Ions in Matter (SRIM) [16] Monte Carlo computer code with a threshold displacement energy, E_d, of 15 eV [17], a density of 2.329 g.cm^{-3}, sample thickness of 50 nm and an angle between the incident ion and specimen normal of 30° to match the experimental conditions. Ion fluences were converted to average displacements per atom across the thickness of the specimen (assumed to be 50 nm) using the output values from the SRIM calculation of 11 disp./He and 1853 disp./Xe. The relationship dpa = (disp. per ion * fluence) / (number of atoms in the irradiation volume) was then used to convert fluence to dpa. In both irradiations, the ion beam flux was adjusted to maintain a damage injection rate of 2×10^{-3} displacements per atom (dpa) per second with the dpa per ion calculated using the Monte-Carlo code SRIM. An electron accelerating voltage of 100 keV was utilised in order to minimise electron-beam-induced recovery [10, 11]. The electron beam was not incident on the sample during ion irradiation to further reduce electron-beam induced re-crystallisation.

Selected area electron diffraction (SAED) patterns of the same region were taken after each fluence step with identical filament and condenser lens settings. The electron current density was set such that the diffraction spots did not saturate the CCD detector of the Gatan Orius SC200 camera in order to avoid pixel blooming effects. Diffraction patterns were always recorded on the [001] zone axis with samples being re-orientated when necessary. Complete amorphisation was

deemed to have occurred at a fluence when crystalline diffraction spots were no longer visible and an amorphous halo was observed. The ion irradiation was then continued to around 1.5 times the fluence at which diffraction spots were no longer detected in order to ensure that complete amorphisation was achieved. Line scans from the 220 to the $\bar{2}\bar{2}0$ reflections were taken from the diffraction patterns and the background intensity, I_B, removed by manually fitting to the following equation:

$$I_B = a + bx e^{-cx} \quad (4)$$

where a, b and c are constants and x is the position along the line scan. When the <220> spots were too faint to locate, line scans were taken from the locations relative to the 000 central spot at which the spots had last been observed. After background removal, the intensities in the amorphous halos were then measured and converted to an amorphous-ring intensity normalised to the fully-amorphous ring intensity [1, 2].

It is assumed that the amorphous ring intensity is linearly proportional to the amorphous fraction given that: the exposure time for the capture of each SAED pattern was kept the same; measurements of the amorphous ring intensity were made within the linear response of the CCD detector; the same area of the sample and crystallographic orientation were used for the capture of all SAED patterns; no significant sputtering was observed from the thin edges of the TEM samples; and the electron beam illumination conditions were kept constant.

SAED patterns from both the He and Xe irradiations are shown in Figure 1. Both irradiations demonstrate similar features: the diffraction patterns show that the material is initially single-crystal with only the reflections normally present in the [001] diffraction pattern being present. Subsequent patterns then show the appearance of an amorphous halo observed concurrently with the diffraction spots. Further ion irradiation causes the crystalline spots to

disappear completely with only the amorphous halo remaining. This demonstrates that both the crystalline and amorphous phases co-exist during the irradiation induced transition from the crystalline to amorphous phase.

That said, the ion fluence and the damage levels at which the material is rendered amorphous are significantly different in the two cases. During Xe irradiation the material is rendered completely amorphous at a fluence of 6.7×10^{13} ion.cm^{-2} (0.50 dpa). Whilst the crystalline-to-amorphous transition for the He irradiation occurred at a much greater fluence of 2.7×10^{17} ions.cm^{-2} (11.9 dpa).

Observations from Figure 1 indicate that in both irradiations, the amorphisation proceeds via a heterogeneous nucleation process rather than the homogeneous process that is generally accepted for low mass ions such as He [2]. However, a greater fluence by four-orders of magnitude (and over two-orders of magnitude greater in dpa) is required to achieve complete amorphisation in the case of He relative to Xe.

In order to explore the amorphisation processes in more detail, it is possible to look at the way in which the amorphous fraction, as a function of fluence or dpa, increases during irradiation as shown in Figure 2. Comparison of the two curves reveals fundamental differences in the shape of the fitted curves and in particular the gradient of the near-linear section. The amorphous fraction as a function of ion fluence for the Xe ion irradiation (Figure 2b) increases rapidly from the first irradiation step before tending asymptotically to saturation at complete amorphisation at fluences above 6.7×10^{13} ions.cm^{-2}. This curve is characteristic of a single-hit, direct-amorphisation process [2] described by Equation 1 with $m = 1$ (as expected [8] under the Xe ion irradiation conditions used here) and $V = 200$ nm^3.ion^{-1}. This corresponds to a spherical amorphised volume ~7.2 nm in diameter – comparable to the volume disordered by a dense collision cascade.

Examination of the amorphous fraction curve for the He ion irradiation shows that the amorphous material initially accumulates at a relatively-slow rate, then increases before saturation towards a fluence of 2.7×10^{17} ions.cm^{-2}. This curve shape is characteristic of a multi-hit heterogeneous amorphisation mechanism in which the gradient indicates the number of cascade overlaps, m, required to render a given volume amorphous. In the case of the He ion irradiation presented here, the curve was fitted to $m = 4$ and $= 0.13$ nm^3.ion^{-1} indicating that on average four cascades must overlap in order to render a region amorphous. Physically this represents the size of the small residual volume at the core of the average cascade and is equivalent to ~6.5 atoms. Damage produced at this level is sufficiently low enough that it would not be possible to image the damage cascade within the electron microscope, and as such only those with higher than this average damage levels will be imaged.

Whilst the AJM equation given in Equation 3 has been used to successfully describe the ion-beam-induced amorphisation of Si, it is not applied here as the primary focus of this study is to understand the role of cascade overlap that is not described in the AJM model.

The results presented demonstrate that during room temperature low energy He ion irradiation the silicon substrate amorphises via a heterogeneous mechanism that on average requires four separate cascades to spatially overlap with each other. It should be noted that this value is likely to be an underestimation due to the presence of the free surfaces in a TEM sample which may lead to an enhancement of amorphisation processes relative to the bulk case [19].

This study shows that there are fundamental differences between the two irradiations even though the damage injection rate was equivalent in both cases. In the Xe irradiation, the energy transfer between the incoming energetic ion and a lattice atom during an atomic collision will, in general, be sufficient to permanently displace the lattice atom. This results in dense collision

cascades in which large amounts of energy can be deposited in a relatively small volume creating amorphous pockets. Conversely, when irradiating with He ions at this energy, the energy transfer will displace a much smaller number of lattice atoms per incident ion. As a result, irradiating with He produces only dilute cascades with insufficient damage to produce amorphous pockets in a single hit. However, with continued irradiation, the probability of collision cascade overlap increases and as more cascades begin to overlap the damage within the overlapping volumes increases in a cumulative manner until it becomes amorphous.

Another factor that should be considered is the electronic-to-nuclear energy loss ratio, S_n/S_e. This ratio can be calculated using SRIM and the data are given in Table 1. Examining the conditions used in these experiments, energy loss ratios of 17.43 and 0.09 are obtained for the He and Xe irradiations, respectively. Given that the energy loss ratio can have a significant impact on the defect formation and stability in ionic-covalent systems [20, 21], this could play a role in the amorphisation kinetics of ion irradiated Si. The two irradiations performed in these experiments have significantly different energy loss mechanisms: Xe being predominantly nuclear and He predominantly electronic. Whilst this affects the concentration of defects contained within the collision cascade volume (as discussed above), it may also significantly impact the defect recovery within these cascades. During the He (light-ion) irradiation, the majority of energy loss is through the electronic system in which the energy is effectively dissipated through bond excitation. That is, the electronic energy transfer in the He irradiation performed here is expected to be insufficient to generate damage itself, but may facilitate damage recovery through electron-phonon coupling processes [20, 21].

There are therefore at least two competing factors in the ion irradiation induced amorphisation of silicon: the direct nuclear displacement damage and the recovery driven by the

electronic processes. During the 80 keV Xe ion irradiation, the low rate of electronic energy loss relative to nuclear energy loss results in dense collision cascades that cause direct amorphisation within the cascade volume. Compare this with the 30 keV He irradiation, in which, the nuclear energy transfer creates less dense damage within the confines of the cascade volume and also the degree of damage within the cascade may be reduced through repair mechanisms driven by the electronic energy loss processes. Furthermore cascades are required to undergo multiple overlaps to increase the damage levels to a state at which the Si becomes amorphous. In the irradiations performed in these experiments, on average four He-induced collision cascades are required to overlap to render the material amorphous.

In conclusion, TEM combined with *in situ* ion irradiation has been used to directly observe and compare the amorphisation of silicon at room temperature by Xe versus He ion irradiation. Analysis of the diffraction patterns and derived amorphous-fraction curves revealed that the loss of crystallinity in both irradiations occurred through a heterogeneous nucleation mechanism. However, with the Xe irradiation, each ion creates on average a damage volume that is amorphous whereas on average four atomic collision cascades are required to overlap to render a damage volume amorphous during the He irradiation. Examining the possible energy loss mechanisms, the Xe irradiation produces dense cascades due to the significant kinetic energy transfer and low electronic energy loss whilst the He irradiations result in relatively inefficient kinetic energy transfer and stronger electronic energy loss processes producing dilute cascades. The relatively high proportion of energy deposited into the electronic system may also lead to a degree of enhanced dynamic recovery necessitating an increased number of cascade overlaps to amorphise the material.

The MIAMI facility was funded by EPSRC under grant reference EP/E017266/1. Work at Oak Ridge National Laboratory was supported by the U.S. Department of Energy, Office of Science, Basic Energy Sciences, Materials Science and Engineering Division.

[1] J. A. Hinks, P. D. Edmondson, J. Appl. Phys. 111 (2012) 053510-053517.
[2] P. D. Edmondson, D. J. Riley, R. C. Birtcher, S. E. Donnelly, J. Appl. Phys. 106 (2009) 043505-043508.
[3] W. J. Weber, Nuclear Instruments and Methods in Physics Research Section B: Beam Interactions with Materials and Atoms 166-167 (2000) 98-106.
[4] F. L. Vook, H. J. Stein, Rad. Effects 2 (1969) 23.
[5] M. L. Swanson, J. R. Parsons, C. W. Hoelke, Rad. Effects 9 (1971) 249.
[6] L. T. Chadderton, Rad. Effects 8 (1971) 77-86.
[7] F. F. Morehead, B. L. Crowder, Rad. Effects 6 (1970) 27-32.
[8] J. F. Gibbons, Proceedings of the IEEE 60 (1972) 1062-1096.
[9] S. E. Donnelly, R. C. Birtcher, V. M. Vishnyakov, P. D. Edmondson, G. Carter, Nuclear Instruments and Methods in Physics Research Section B: Beam Interactions with Materials and Atoms 242 (2006) 595-597.
[10] I. Jenčič, M. W. Bench, I. M. Robertson, M. A. Kirk, J. Appl. Phys. 78 (1995) 974-982.
[11] I. Jenčič, I. M. Robertson, Materials Science in Semiconductor Processing 3 (2000) 311-315.
[12] S. E. Donnelly, R. C. Birtcher, V. M. Vishnyakov, G. Carter, Appl. Phys. Lett. 82 (2003) 1860-1862.
[13] B. Canut, M. Fallavier, O. Marty, S. M. M. Ramos, Nuclear Instruments and Methods in Physics Research Section B: Beam Interactions with Materials and Atoms 164-165 (2000) 396-400.
[14] A. I. Titov, S. O. Kucheyev, V. S. Belyakov, A. Y. Azarov, J. Appl. Phys. 90 (2001) 3867-3872.
[15] J. A. Hinks, J. A. van den Berg, S. E. Donnelly, Journal of Vacuum Science & Technology A: Vacuum, Surfaces, and Films 29 (2011) 021003-021006.
[16] J. F. Ziegler, J. Appl. Phys. 85 (1999) 1249-1272.
[17] P. D. Edmondson, W. J. Weber, F. Namavar, Y. Zhang, J. Nucl. Mater. 422 (2012) 86-91.
[18] K. Nordlund, M. Ghaly, R. S. Averback, M. Caturla, T. Diaz de la Rubia, J. Tarus, Physical Review B 57 (1998) 7556-7570.
[19] J. S. Williams, M. J. Conway, J. Wong-Leung, P. N. K. Deenapanray, M. Petravic, R. A. Brown, D. J. Eaglesham, D. C. Jacobson, Appl. Phys. Lett. 75 (1999) 2424-2426.
[20] Y. Zhang, D. S. Aidhy, T. Varga, S. Moll, P. D. Edmondson, F. Namavar, K. Jin, C. N. Ostrouchov, W. J. Weber, Physical Chemistry Chemical Physics 16 (2014) 8051-8059.
[21] Y. Zhang, T. Varga, M. Ishimaru, P. D. Edmondson, H. Xue, P. Liu, S. Moll, F. Namavar,

C. Hardiman, S. Shannon, W. J. Weber, Nuclear Instruments and Methods in Physics Research Section B: Beam Interactions with Materials and Atoms 327 (2014) 33-43.

Table 1: Energy loss values during He and Xe ion irradiation of Si (50 nm thick), at an angle of 30° between incident ion and sample surface normal obtained from SRIM calculations.

Ion	Energy (keV)	S_n (eV/nm)	S_e (eV/nm)	S_e/S_n
He	30	100.10	5.74	17.43
Xe	80	159.30	1683.00	0.09

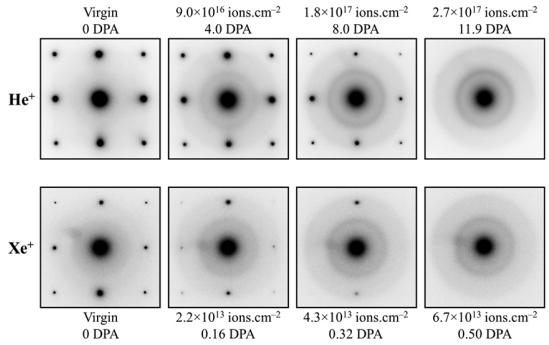

Figure 1: Sequences showing the [001] diffraction pattern during He (top) and Xe (bottom) ion-irradiation-induced amorphisation of silicon.

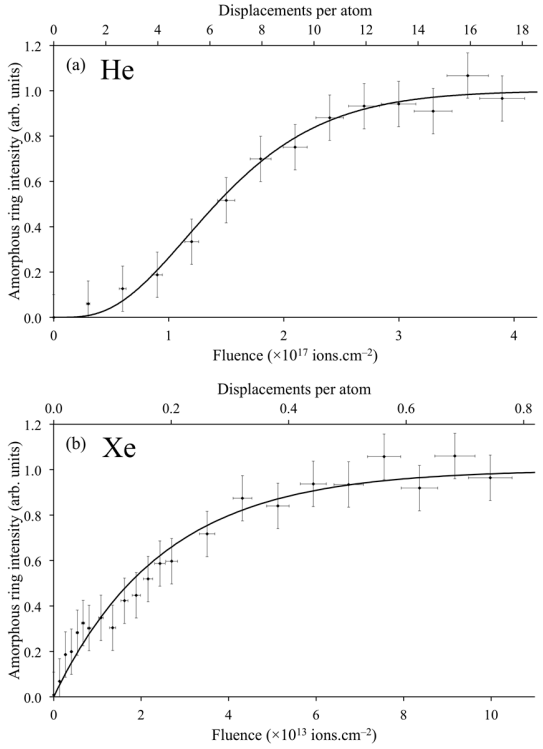

Figure 2: Plots of the amorphous ring intensity against fluence and dpa for Si under (a) He ion irradiation and (b) Xe ion irradiation. The fitted curves correspond to a modified Gibbons model [8] for a m=4 amorphisation process for He and m=1 for Xe.